LETTER

Impact of Shadowing Correlation on Reverse Link Capacity of DS-CDMA Cellular System

Arif JUNAIDI[†a)], ***Student Member***, **Eisuke KUDOH**[†b)], ***and*** **Fumiyuki ADACHI**[†c)], ***Members***

SUMMARY Independent shadowing losses are often assumed for evaluating the link capacity of direct sequence code division multiple access (DS-CDMA) cellular system. However, shadowing losses may be partially correlated since the obstacles surrounding a mobile station block similarly the desired signal and the interfering signals. In this letter, we discuss how the shadowing correlation impacts the reverse link capacity of a power-controlled DS-CDMA cellular system, by numerical analysis.

key words: *DS-CDMA cellular system, reverse link capacity, shadowing correlation*

1. Introduction

Evaluating the link capacity is an important technical issue to design a cellular system. Independent shadowing losses are often assumed for evaluating the link capacity of direct sequence code division multiple access (DS-CDMA) cellular systems. However, shadowing losses may be partially correlated since the obstacles surrounding a mobile station (MS) block similarly the desired signal and the interfering signals. The impact of shadowing correlation on the spectrum efficiency of a power-controlled FDMA system is discussed in [1], where the shadowing correlation is assumed to be independent of the geographical locations of an MS and a base station (BS). However, an obstacle could be likely responsible of shadowing two different links between an MS and two different BSs [2]–[6]. A geographical location-dependent shadowing correlation model was proposed in [3]–[6], where the correlation is given as a function of the angular difference between the two links. In this letter, we use a modified shadowing correlation model and numerically investigate how the shadowing correlation impacts the reverse link capacity of a power-controlled DS-CDMA cellular system.

2. Shadowing Correlation Model

Figure 1 illustrates the geographical locations of an interfering MS and two different BSs. In Fig. 1, b denotes the BS index and $j(b)$ denotes the j-th MS connected to the b-th BS. Without lose of generality, we assume that the 0(0)-th MS is the desired MS and is communicating with the 0-th BS. $\eta_{j(b),0}$ is the shadowing loss expressed in dB between the $j(b)$-th MS and the 0-th BS and follows a zero-mean Gaussian distribution with a standard deviation σ. In Fig. 1, $\theta_{j(b),0\leftrightarrow b}$ denotes the angular difference between the two links. As $|\theta_{j(b),0\leftrightarrow b}|$ decreases, the same obstacle tends to block both links, and thus a higher shadowing correlation would be observed. We use the following modified correlation model:

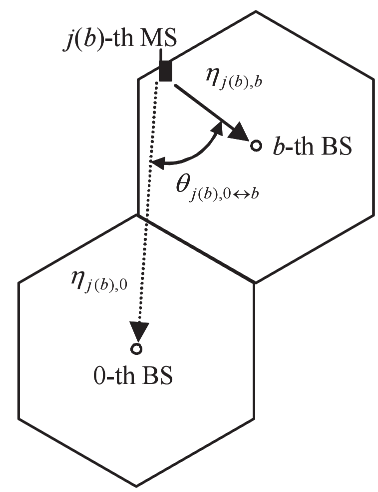

Fig. 1 Geographical locations of an interfering MS and two BSs.

$$\rho_{j(b),0\leftrightarrow b} = \begin{cases} u\cos\left(\dfrac{\theta_{j(b),0\leftrightarrow b}}{w}\right) + v \\ \quad \text{if } -w\times 90^\circ \leq \theta_{j(b),0\leftrightarrow b} \leq w\times 90^\circ \\ v \quad \text{otherwise} \end{cases}, \quad (1)$$

where u, v and w are positive parameters with $u+v \leq 1$. In the correlation model of Refs. [3] and [4], the fading correlation is constant for $|\theta| > 90^\circ$. However, in a real environment, the range of θ in which the shadowing correlation is affected by obstacles may not necessarily be limited to 90°. If big obstacles exist, the shadowing correlation may change even for $|\theta| > 90^\circ$ [5], [6]. However, if obstacles are relatively small, the obstacles may affect the shadowing correlation only in a range of small $|\theta|$ (i.e. $|\theta| \leq 90^\circ$). Therefore, the parameter "w" is introduced to control the range of θ in which the obstacles affect the shadowing correlation.

Manuscript received March 27, 2006.
Manuscript revised July 1, 2006.
†The authors are with the Dept. of Electrical and Communication Engineering, Graduate School of Engineering, Tohoku University, Sendai-shi, 980-8579 Japan.
a) E-mail: arif@mobile.ecei.tohoku.ac.jp
b) E-mail: kudoh@ecei.tohoku.ac.jp
c) E-mail: adachi@ecei.tohoku.ac.jp
DOI: 10.1093/ietcom/e89–b.12.3483

3. Received SINR Expression

Each user is connected to the BS with the largest local average link gain. Assuming an L-path Rayleigh fading channel, M-branch antenna diversity and L-finger rake combining with ideal maximal ratio combining (MRC) are considered. The received signal-to-noise power ratio (SNR) after rake combining is given by

$$SNR = \left(\frac{T}{N_0}\right) P_{0(0)} A_{0(0),0} \sum_{m=0}^{M-1} \sum_{l=0}^{L-1} \left|\xi_{0(0),0}(m,l)\right|^2, \quad (2)$$

where $P_{0(0)}$ is the transmit power, T the symbol duration, N_0 the single-sided power spectrum density of the additive white Gaussian noise (AWGN), $\xi_{j(b),0}(m,l)$ the path gain of the l-th path associated with the m-th antenna ($l = 0 \sim L-1$, $m = 0 \sim M-1$), and

$$A_{j(b),0} = a_{j(b),0}^{-\alpha} 10^{-\eta_{j(b),0}/10} \quad (3)$$

is the local average link gain between the $j(b)$-th MS and the 0-th BS with $a_{j(b),0}$ being the distance between the $j(b)$-th MS and the 0-th BS, normalized by the cell radius, and α is the path loss exponent.

Transmit power control (TPC) is an indispensable technique to mitigate the near-far problem. Assuming the signal-to-noise power ratio (SNR)-based ideal fast TPC, the transmit power $P_{0(0)}$ of the 0(0)-th MS is given by

$$P_{0(0)} = \left(\frac{N_0}{T}\right) \frac{SNR_{\text{target}}}{A_{0(0),0} \sum_{m=0}^{M-1} \sum_{l=0}^{L-1} \left|\xi_{0(0),0}(m,l)\right|^2}, \quad (4)$$

where SNR_{target} is the target SNR. The rake combiner output is the sum of the inter-path interference (IPI), multi-user interference (MUI), inter-cell interference (ICI), and noise components (however, in the following, the IPI component is ignored since we assume a large spreading factor SF). Assuming a Rayleigh fading channel, this sum can be treated as a complex valued Gaussian variable [7]. Hence, the signal-to-interference plus noise power ratio (SINR) Λ_0 required for a certain bit error rate (BER) P_e which can be determined using [8]

$$P_e = \frac{1}{2} erfc \sqrt{\frac{\Lambda_0}{2}}. \quad (5)$$

As in [9], the interference rise factor χ is introduced. SNR_{target} is set as

$$SNR_{\text{target}} = \chi \Lambda_0. \quad (6)$$

Following [10], the received SINR Λ can be obtained as (only the result is shown here for the sake of brevity)

$$\Lambda = SF \left(\frac{J-1}{M} + \frac{L}{ML-1} \sum_{b=1}^{N_C} \sum_{j=0}^{J-1} \frac{A_{j(b),0}}{A_{j(b),b}} + \frac{SF}{\chi \Lambda_0} \right)^{-1}, \quad (7)$$

where SF is the spreading factor, J the number of MSs per cell and N_C the number of interfering cells considered in the performance evaluation. We have assumed that J MSs are communicating with every BS.

4. Outage Probability

The outage probability Q is the probability of the received SINR being less than the required SINR Λ_0. The second term $I = \left(\frac{L}{ML-1}\right) \sum_{b=1}^{N_C} \sum_{j=0}^{J-1} A_{j(b),0}/A_{j(b),b}$ in the round bracket of Eq. (7) is the sum of $N_C \cdot J$ log-normally distributed random variables and can be approximated as another log-normally distributed random variable [11], [12]. Therefore, we use

$$I \approx 10^{\psi/10} = \exp(\beta\psi), \quad (8)$$

where $\beta = (\log 10)/10$ and ψ is a Gaussian random variable with mean μ_ψ and variance σ_ψ^2. μ_ψ and σ_ψ^2 are obtained by using the mean μ_I and variance σ_I^2 of I as [11]

$$\begin{cases} \mu_\psi = \dfrac{1}{\beta}\left[\log \mu_I - \dfrac{\beta^2 \sigma_\psi^2}{2}\right] \\ \sigma_\psi^2 = \dfrac{1}{\beta^2} \log\left[\dfrac{\sigma_I^2}{\mu_I^2} + 1\right] \end{cases}. \quad (9)$$

Letting $I(x, y)$ be the interference power from an MS located at co-ordinate (x, y), I is given as

$$I = \frac{J}{Z} \iint I(x,y)\, dxdy, \quad (10)$$

where Z is the area of the cell (i.e., J/Z is the user density). μ_I and σ_I^2 are numerically evaluated using

$$\begin{cases} \mu_I = \dfrac{J}{Z} \iint E[I(x,y)]\, dxdy \\ \sigma_I^2 = \left(\dfrac{J}{Z}\right)^2 E\left[\left(\iint I(x,y)\, dxdy\right)^2\right] - \mu_I^2 \end{cases}. \quad (11)$$

The outage probability Q is given as

$$\begin{aligned} Q &= \text{Prob } [\Lambda \le \Lambda_0] = \text{Prob } [\psi \ge \lambda] \\ &= \Phi\left(\frac{\mu_\psi - \lambda}{\sqrt{2}\sigma_\psi}\right), \end{aligned} \quad (12)$$

where

$$\lambda = 10 \log_{10}\left[\frac{SF}{\Lambda_0}\left(1 - \frac{1}{\chi}\right) - \frac{J-1}{M}\right] \quad (13)$$

and $\Phi(x) = (1/\sqrt{\pi}) \int_x^\infty \exp(-t^2)dt$ is the complementary error function. The link capacity C is defined as the maximum number of users that satisfies the allowable outage probability Q_0, i.e.,

$$C = \arg \max_J [Q \le Q_0]. \quad (14)$$

Table 1 Numerical and simulation conditions.

Modulation	QPSK
Spreading factor	SF=64
Shadowing standard deviation	σ=6dB
Path loss exponent	α=3.5
No. of paths	L=2
No. of interfering cells	N_C=18
Interference rise factor	χ=10 dB
No. of diversity antennas	M=2
Required SINR	Λ_0=7.3dB (for P_e=10^{-2})

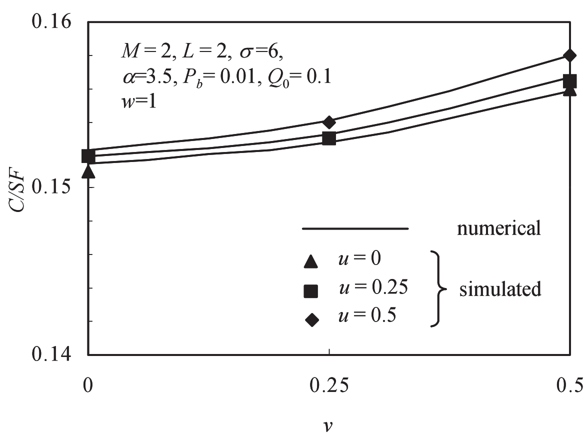

Fig. 2 Normalized link capacity C/SF as a function of v.

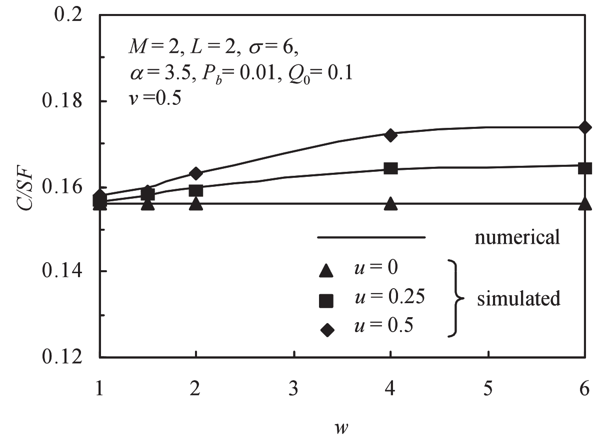

Fig. 3 Normalized link capacity C/SF as a function of w.

5. Numerical and Simulation Results

The numerical and simulation conditions are shown in Table 1. In the computer simulation, J MSs uniformly distributed in each cell are generated. Then, the path loss and shadowing loss associated with each MS are generated and the communicating BS is selected for each MS based on the local average link gain. Therefore, the number of MSs communicating with each BS is not necessarily equal to J in the computer simulation, while, in the numerical calculation, the number of MSs communicating with each BS is equal to J. The received SINR Λ is computed using Eq. (7) and compared to the required SINR Λ_0. The outage occurs if Λ is smaller than Λ_0. This trial is repeated a sufficient number of times to obtain the outage probability Q.

Figure 2 shows the normalized link capacity C/SF as a function of v. It is seen that as v increases, the link capacity C also increases. As understood from Eq. (1), as the value of v increases, the shadowing correlation ρ increases; this suggests that the link capacity increases as ρ increases, similar to the case of an FDMA cellular system [9]. Figure 3 shows the normalized link capacity C/SF as a function of w. If $u > 0$, the link capacity increases as w increases. It can be seen from Figs. 2 and 3 that the link capacity is affected not only by u and v but also by w (which is not considered in Refs. [3] and [4]). In Figs. 2 and 3, the computer simulation results are also plotted. A good agreement is seen between the numerical and computer simulation results. This suggests that the assumption of J MSs being communicating with each BS in the numerical calculation gives an almost negligible error in the capacity evaluation.

6. Conclusion

In this letter, we investigated the impact of shadowing correlation on the reverse link capacity of a power-controlled DS-CDMA cellular system. We used the shadowing correlation model given by Eq. (1). It was shown that the link capacity is affected not only by u and v but also by w. Therefore, an accurate shadowing correlation model is necessary for the capacity estimation.

References

[1] K. Sawa, E. Kudoh, and F. Adachi, "Impact of shadowing correlation on spectrum efficiency of a power controlled cellular systems," IEICE Trans. Commun., vol.E87-B, no.7, pp.1964–1969, July 2004.

[2] M. Gudmundson, "Correlation model for shadow fading in mobile radio system," Electron. Lett., vol.27, no.23, pp.2145–2146, Nov. 1991.

[3] F. Graziosi and F. Santucci, "A general correlation model for shadow fading in mobile radio systems," IEEE Commun. Lett., vol.6, no.3, pp.102–104, March 2002.

[4] F. Graziosi, M. Pratesi, M. Ruggieri, and F. Santucci, "A multicell model of handover initiation in mobile cellular networks," IEEE Trans. Veh. Technol., vol.48, no.3, pp.802–814, May 1999.

[5] V. Graziano, "Propagation correlation at 900 MHz," IEEE Trans. Veh. Technol., vol.27, no.4, pp.182–189, Nov. 1978.

[6] T. Fujii, "Reduction of mobile radio co-channel Interference by adaptive transmitter power control in correlated shadowing condition," IEICE Trans. Commun. (Japanese Edition), vol.J75-B-II, no.12, pp.906–917, Dec. 1992.

[7] W.C. Jakes, Jr., ed., Microwave Mobile Communication, John Wiley, 1974.

[8] J.G. Proakis, Digital Communications, 4th ed., McGraw Hill, New York, 2000.

[9] F. Adachi, A. Katoh, and D. Garg, "Joint effect of transmit power control and antenna diversity on spectrum efficiency of a cellular system," IEICE Trans. Commun., vol.E85-B, no.5, pp.919–928, May 2002.

[10] D.K. Kim and F. Adachi, "Capacity estimation for overlaid multiband CDMA systems with SIR-based power control," IEICE Trans.

Commun., vol.E87-B, no.7, pp.452–464, July 2004.

[11] L. Fenton, "The sum of log-normal probability distributions in scatter transmission system," IEEE Trans. Commun. Syst., vol.CS-8, no.1, pp.57–67, March 1960.

[12] F. Santucci, "A general analysis of signal strength handover algorithm with cochannel interference," IEEE Trans. Commun., vol.48, no.2, pp.231–241, Feb. 2000.